RADIO IMAGING OF FLARES
(Invited)

George A. Dulk

Department of Astrophysical, Planetary and Atmospheric Sciences
University of Colorado, Boulder, CO 80309, U.S.A.

ABSTRACT

High resolution (arcseconds to tens of arcseconds) mapping of solar microwave bursts has recently been achieved. I review the properties of the radio images that have been reported to now and, so far as possible, the relation of the radio sources to X-ray observations of the same flares.

I. INTRODUCTION

One of the most important advances during the past solar maximum was the development of the capability of imaging flare emissions with a resolution of some tens of arcseconds to less than one arcsecond, i.e., adequate to resolve almost all sources. This capability was achieved in one dimension in Nagoya, Japan at 35 GHz, Nobeyama, Japan at 17 GHz, Westerbork, Netherlands at 1.4 and 5 GHz, and in two dimensions at the VLA in the USA at 1.4, 5, 15, and 22 GHz. Because Westerbork and the VLA are general purpose instruments, only a small fraction of their time is used for solar studies so the number of flares observed by them has been severely limited; nevertheless they obtained a number of very important results, some of which will be described here.

Of particular relevance to this workshop is the fact that radio waves in the decimetric-centimetric band emanate from the same populations of energetic electrons that produce soft and/or hard X rays. Time profiles ("light curves") of radio bursts are nearly identical to those of X-ray bursts even on time scales of 1 s or less. In general the form and duration of the light curves vary with radio frequency and X-ray energy, with the curves of the higher frequency radio waves corresponding better with those of the higher energy X rays; some aspects of the correlations and spectral properties will be discussed by G. Hurford at this meeting. Because of this high temporal correlation, one would expect that images made at radio and X-ray wavelengths would also be similar, with source structure at some tens of GHz resembling that at hundreds of keV, structure at a few GHz resembling that at tens of keV, and structure near 1 GHz resembling that at a few keV. However, verification of the expectation has not been possible because (1) no X-ray images have been obtained at energies $\gtrsim$30 keV, (2) the number of flares imaged in radio waves has been small and those with simultaneous X-ray imaging even smaller, and (3) in almost all cases of joint coverage the frequency of the radio image has not matched the energy of the X-ray image. Only in the event described by Kundu et al. (1984) was there near compatibility – 5 GHz radio and 16 to 30 keV X rays, and then the images were indeed very similar.

In addition to mapping the intensity of radiation, it is possible at radio frequencies to make maps in both right-hand (RH) and left-hand (LH) polarization, or equivalently, in Stokes parameter V = RH – LH or degree of circular polarization r_c = V/I = (RH - LH)/(RH + LH). At the higher frequencies where the source is optically thin, the sense of circular polarization

immediately gives the direction of the magnetic field in the source region, with RH and LH polarizations implying that the longitudinal component of field is directed toward and away from the observer respectively. Here it is assumed that gyrosynchrotron radiation is the radio emission mechanism of the relevant bursts, an assumption that is well substantiated by both theory and observations. With additional information on electron energies, sometimes available from hard X-ray observations, it is also possible to infer the magnetic field strength in the source region. Typical values are in the range of 100 to 500 Gauss.

In the remainder of this paper I will describe the main results achieved from radio imaging of flares by showing some examples of the better-observed flares or ones illustrating the points most clearly. Two cautions are necessary: the first is the usual one that flares differ so much in their temporal, morphological, and spectral characteristics that it is difficult to make deductions that apply to more than a subclass of flares, and second is the point that I can illustrate only a handful of cases, so the selection is both incomplete and biased towards flares observed in two dimensions, i.e., with the VLA. The reader can find more illustrations and implications in reviews by Marsh and Hurford (1982), Kundu and Vlahos (1982), Kundu (1982), and Canfield et al. (1985), and in detailed reports by Allisandrakis and Kundu (1978), Kattenberg (1981), Kundu, Bobrowsky, and Velusamy (1981), Marsh et al. (1981), Kundu et al. (1982), Ohki et al. (1982), Velusamy and Kundu (1982), Duijveman and Hoyng (1983), Dulk, Bastian, and Hurford (1983), Hoyng et al. (1983), Kai et al. (1983), Kawabata, Ogawa, and Suzuki (1983), Lang and Willson (1983), Tsuneta et al. (1983), Willson (1983), Kundu et al. (1984), Lang and Willson (1984), Dulk, Bastian, and Kane (1985), and Nakajima et al. (1985).

II. DISCUSSION OF INDIVIDUAL EVENTS AND THEIR IMPLICATIONS

Event of 5 November 1980, 2226 UT

Hoyng et al. (1983) and Duijveman and Hoyng (1983) described the hard X-ray and radio imaging of this flare, a relatively weak one that preceded by about 7 min a more intense flare much described in the literature but for which no radio images are available. As seen in Figure 1 the flare lasted only a few minutes and had three peaks, the last was visible mainly in softer X rays and was not evident at 9.4 or 15 GHz; the first two peaks were not properly resolved with 10 s time resolution of the VLA. The upper-right part of Figure 1 shows the flaring region at the times of the first two peaks with the magnetic neutral line, the 15 GHz radio sources, and the HXIS pixels in which there were significant numbers of counts (shaded) in the 16 to 30 keV range. The 15 GHz sources are seen to straddle the neutral line of the magnetic field; this is a general rule to which there are only a few exceptions. The sources are very small, less than about 5 $''$ in extent; this also is common, with sizes averaging about 3 $''$ at 15 GHz, 10 $''$ at 5 GHz, and 30 $''$ at 1.4 GHz. Because of the weakness of the flare, few counts were recorded in the HXIS 16 to 30 keV channel. During the first peak (top right), two separated pixels had a significant number of counts, probably near footpoints of loops arching over the neutral line. During peak 2 one of the two pixels with significant counts was the central one coinciding with the radio source, but its X-ray spectrum was probably softer than that of the outer pixel. Peak 3 was also largely from the central pixel, and its spectrum was softer yet.

The bottom part of Figure 1 shows the location of the RH and LH radio sources of peak 2 relative to the neutral line and the Hα bright features. The neutral line as drawn may be misplaced by a few arcseconds, and its probable location is between the two ribbons of the flare. In any case the RH and LH radio sources are predominantly on the sides of + and - polarity, respectively. In addition, the radio source straddles the region of the brightest Hα kernels. These also are common, nearly ubiquitous features of radio images of flares.

The 15 GHz brightness temperature in RH polarization during peak 2 was 9.4 x 10^8 K, and the source was optically thick or nearly so. From this it follows that the average energy of the emitting electrons was $\gtrsim$100 keV; in fact, the HXRBS experiment observed X rays to about 300 keV. From the degree of circular polarization and the radio spectrum, the magnetic field strength in the 15 GHz source was estimated to be about 500 Gauss. With the density estimated from X-ray data to be about 3 x 10^{10} cm^{-3}, the plasma beta was $\beta \approx 10^{-2}$, showing a dominance of magnetic energy density in the source region.

Event of 24 June 1980, 1522 UT

Kundu et al. (1984) described the hard X-ray and VLA imaging at 5 GHz of this flare. It was located within 30 deg of disk center and was of importance SB in Hα and M1 in soft X rays. Figure 2 shows light curves in soft and hard X rays; the duration of the latter was only about 3 min. Figure 2 also shows the relationship of the 5 GHz radio source to the soft and hard X-ray sources and the off-band Hα features. Several points are notable: (1) The 5 GHz source size, about 10 $''$ x 20 $''$, was only slightly smaller than the hard X-ray source. (2) The radio and hard X-ray sources overlapped but seemed to be slightly displaced from each other; however, this might not be significant in view of possible alignment errors. (3) The radio source lay near the extremity of the off-band Hα brightening and it is not clear what its relation was to the magnetic field. However, on polarization maps (not shown) the northern and southern parts of the radio source were polarized in the LH and RH sense, respectively. (4) The soft X-ray source was considerably larger (>60 $''$) than either the hard X-ray or radio source and its center was displaced from them. (5) After the radio and hard X-radiation had ceased, the soft X-radiation covered a huge area that generally coincided with but even exceeded the extent of the Hα brightenings.

Event of 12 June 1980, 1340 UT

Willson (1983) described this impulsive event which was observed with the VLA at its lowest frequency of 1.4 GHz. While the overall flare lasted several minutes, we describe only the first of three peaks, one which lasted only about 10 to 20 s. Figure 3 shows the VLA images at three times, 10 s apart. The left panel shows the region just before the burst or possibly at its leading edge, with the radiation being slightly RH polarized. The middle panel is for the next 10 s interval, the one containing the burst. The source size was about 30 $''$, considerably larger than is typical of 5 or 15 GHz sources. The brightness temperature was only moderate, 1.5 x 10^8 K. The polarization had changed dramatically from the previous 10 s map, being RH polarized only on the eastern edge while the brightest part was nearly 100% LH polarized. The right panel shows the region 10 s later yet, during burst decay, when the polarization had returned nearly to its pre-burst state.

In the absence of further information it is not possible to decide with confidence the origin of this burst. At decimetric wavelengths not all bursts are due to the same gyrosynchrotron mechanism responsible for the 15 and 5 GHz radiation of the events described previously. Plasma radiation and cyclotron maser radiation are also known to occur near 1.4 GHz.

Event of 22 November 1981, 1743 UT

The events described above involved flares on the disk. This allows the positions of sources to be related to magnetic and Hα features but prevents any direct measurements of source altitudes. From stereo observations from two spacecraft of X-ray bursts, Kane et al. (1979, 1982) have established that impulsive hard X-ray sources are located at very low altitudes,

<2500 km, which is consistent with the belief that they are at the footpoints of magnetic loops. If images are made of flares near the limb, it is possible, at least in principle, to measure directly the source altitudes.

To date only one such flare has been reported. Dulk, Bastian, and Kane (1985) made simultaneous observations at 4.9 and 15 GHz of a flare at 85 deg longitude. The results are summarized in Figure 4. The light curves at the upper left show a weak, impulsive flare with two peaks. For the first peak, the profiles at the two radio frequencies are similar to each other and to that of the 12 to 20 keV X rays (for this burst the highest energy range with enough counts to give a reliable profile). The three middle panels show the radio sources at three times: early in the rise, the first peak, and the second peak. As usual the 15 GHz source is smaller than the 4.9 GHz source, but surprisingly the sources are not cospatial, a fact that would not have been suspected from the light curves alone. There is little or no 4.9 GHz radiation from the main part of the 15 GHz source and vice versa. The upper right panel shows, for the two frequencies, the brightness temperatures near the centers of the two sources. The considerable differences suggest that the emission mechanisms may not be the same in the two sources, and this is borne out in detailed study. On the basis of the combined X-ray and radio data, the northern, 15 GHz source was found to be due to gyrosynchrotron radiation from a small number of ~300 keV electrons, with the 4.9 GHz emission from those electrons being gyroresonantly re-absorbed as it passed over a large sunspot enroute to Earth. The southern, mainly 4.9 GHz source was found to be due to thermal bremsstrahlung from a hot plasma with a temperature ranging from about 5×10^6 K at the periphery to about 20×10^6 K at the center.

The bottom panel of Figure 4 shows the two sources at the time of the burst maximum in relation to the Hα limb and the Hα flare brightenings. In projection the radio sources were at the same height or below the Hα features, probably at an altitude of 3000 km or less. This is rather similar to the height of hard X-ray sources derived by Kane et al. (1979, 1982). Hence, it seems that the fast electrons that emit both the microwaves and hard X-rays in impulsive flares are confined to very low-lying loops or their footpoints.

Event of 8 May 1981, 2200 UT

The events described above were concerned with short-lived impulsive flares, with the evidence indicating that hard X rays come largely from footpoints of low-lying loops and radio waves largely from their central positions. A distinctly different type of flare is typified by a long duration and a large source at a high altitude. An example of this kind of flare occurred on 8 May 1981 and was imaged in soft and hard X-rays by Hinotori, and at 4.9 and 15 GHz by the VLA; it has been described by Ohki et al. (1982) and by Dulk, Bastian, and Hurford (1983). Figure 5 shows two light curves of 15 GHz radiation and one of the 25 to 400 keV X-radiation. Taking into account the linear versus log scales, the 15 GHz profile from Owens Valley is very similar to the hard X-ray profile, but the VLA profile is similar only at the earliest times, before 2220 UT. The VLA profile represents the flux as seen by an interferometer with a fringe spacing of 15.4 arcsecond, the lowest resolution of any antenna pair on that occasion. The decrease in VLA flux after 2220 UT (while it was increasing on the Owens Valley antenna with its 3 ″ resolution) demonstrates that the source increased its size to well above 15 ″. The 4.9 GHz flux recorded by a VLA interferometer with 40 ″ resolution behaved in a similar way, showing that the 4.9 GHz source too was exceptionally large. The lower panel of Figure 5 shows the hard X-ray sources near the time of burst peak and their relation to magnetic and Hα features. Two X-ray sources were present, the main one's size was nearly 1 ′. Also shown in the figure are three small sources that were imaged by the VLA, but they contained only a tiny fraction of the total 15 GHz flux, and their relation to magnetic, hard X-ray, or Hα features is unclear.

A lesson to be learned from this flare is that the VLA is most useful when in a compact configuration, especially if dual frequency observations are desired. When in a widespread configuration there is danger that large-scale structures become invisible and that ambiguities may not allow the positions of small-scale features to be determined.

Event of 29 January 1984, 1825 UT

As reported by Lang and Willson (1984), this flare was imaged at the VLA at several frequencies in the range 1.4 to 1.7 GHz. Figure 6 shows light curves at two frequencies spaced about 0.03 GHz apart, and in the two senses of circular polarization. The burst was weak and the spiky components appeared almost exclusively in RH polarization. There are significant differences in the intensity of a few of the spikes at the two closely spaced frequencies, notably spike 7; this implies that the bandwidth of the spiky radiation was very small, only about 2%.

The upper two panels of Figure 6 shows RH (solid) and LH (dashed) images at the two closely spaced frequencies at the times of peaks 1 to 7. While the structures are seen to be quite similar at the two frequencies, the intensities are not always similar. Further, the LH and RH radiation occurred at distinctly different spatial locations. (It is possible that the polarization of the southern source may have been low, with the corresponding RH contours not visible because of the limited dynamic range of the maps.)

The temporal, spectral, and polarization characteristics of this event suggest that two emission mechanisms were involved, the normal gyrosynchrotron process for the weak, southern source, and the cyclotron maser process for the strong, RH-polarized northern source. The former process is not capable of producing bursts of nearly 100% polarization and narrow bandwidth, but these are typical characteristics of a maser (e.g., Melrose and Dulk, 1982). It would be of great interest to know how hard X rays behaved in the spatial, spectral, and temporal domains at times of microwave spike bursts of the kind illustrated by this event.

III. CONCLUSIONS

In summary, I list some of the general properties derived from radio imaging of flares.

(1) The most common, observed characteristic is that impulsive radio burst sources lie over neutral lines of magnetic fields, and that the source is near the top of one magnetic loop or an arcade, but extending over much of the loop lengths. Radio sources are seldom found only at footpoints.

(2) Radio sources are larger at the lower frequencies; for impulsive flares they are typically 3 $''$ at 15 GHz, 10 $''$ at 5 GHz, and 30 $''$ at 1.4 GHz. However, they are sometimes much larger, especially for extended flares, reaching 1 $'$ or more.

(3) The heights of the impulsive radio sources are quite low, perhaps not much higher than the 2500-km limit found for several hard X-ray bursts. However, this conclusion rests mainly on one limb flare observed with the VLA and requires verification.

(4) The field strengths in the source regions are usually in the range of 100 to 500 Gauss and the plasma beta is usually much less than unity.

(5) Most radio emission at frequencies higher than a few GHz is due to gyrosynchrotron radiation from electrons of energy >100 keV, with the higher frequencies being produced by the more energetic electrons. For γ-ray flares the frequency of peak radio flux extends to 50 GHz or more, with the highest frequency radiation produced by relativistic electrons. Extrapolating the source size versus frequency relation, one would expect the relativistic electrons to occupy a very small volume, $\lesssim 1$ $\mathcal{T}$.

(6) Following the impulsive phases of flares, it is likely that thermal bremsstrahlung from the soft X-ray plasma plays a role in producing the slowly decaying tail of radio emission that is especially evident at the lower frequencies.

(7) At frequencies $\lesssim 3$ GHz cyclotron maser and plasma radiation become increasingly more important. Cyclotron maser emission probably produces the microwave spike bursts observed mostly at $\lesssim 1$ GHz, but occasionally to 3 GHz. In impulsive flares it may also play a major role in the transport of energy from the energy release/hard X-ray/cm burst region into the larger, soft X-ray region (Melrose and Dulk, 1984).

(8) Simultaneous imaging observations in radio and hard X rays have revealed several important phenomena in flares, but their potential has hardly been tapped because X-ray imaging has so far achieved relatively poor spatial resolution compared with radio imaging, and because images have so far been made only at relatively low X-ray energies.

This work was supported in part by NASA's Solar Heliospheric Physics and Solar Terrestrial Theory Programs under grants NSG-7287 and NAGW-91 to the University of Colorado.

REFERENCES

Allissandrakis, C. E. and Kundu, M. R., 1978, *Astrophys. J., 222,* 342.

Canfield, R. C., and 15 co-authors, 1985, Chapter 3 of *Solar Flares: Proc. SMM Workshop,* eds., B. E. Woodgate and M. R. Kundu, in press.

Duijveman, A. and Hoyng, P., 1983, *Solar Phys., 86,* 279.

Dulk, G. A., Bastian, T. S., and Hurford, G. J., 1983, *Solar Phys., 86,* 451.

Dulk, G. A., Bastian, T. S., and Kane, S. R., 1985, *Astrophys. J.,* submitted.

Hoyng, P., Marsh, K. A., Zirin, H., and Dennis, B. R., 1983, *Astrophys. J., 268,* 865.

Kawabata, K., Ogawa, H., and Suzuki, I., 1983, *Solar Phys., 86,* 247.

Kai, K., Nakajima, H., Kosugi, T., and Kane, S. R., 1983, *Solar Phys., 86,* 231.

Kane, S. R., Anderson, K. A. Evans, W. D., Klebesadel, R. W., and Laros, J. G., 1979, *Astrophys. J. (Letters), 233,* L151.

Kane, S. R., Fenimore, E. E., Klebesadel, R. W., and Laros, J. G., 1982, *Astrophys. J. (Letters), 254,* L53.

Kattenberg, A., 1981, Ph.D. Thesis, Univ. of Utrecht.

Kundu, M. R., 1982, *Rep. Prog. Phys., 45,* 1435.

Kundu, M. R. and Vlahos, L., 1982, *Space Sci. Rev., 32,* 405.

Kundu, M. R., Bobrowsky, M., and Velusamy, T., 1981, *Astrophys. J., 251,* 352.

Kundu, M. R., Schmahl, E. J., Velusamy, T., and Vlahos, L., 1982, *Astron. Astrophys., 108,* 188.

Kundu, M. R., Machado, M. E., Erskine, F. T., Rovira, M. G., and Schmahl, E. J., 1984, *Astron. Astrophys., 132,* 241.

Lang, K. R. and Willson, R. F., 1983, *Adv. Space Res., 2,* No. 11, 91.

Lang, K. R. and Willson, R. F., 1984, *Adv. Space Res., 4,* No. 7, 105.

Marsh, K. A., and 6 co-authors, 1981, *Astrophys. J., 251,* 797.

Marsh, K. A. and Hurford, G. J., 1982, *Ann. Rev. Astron. Astrophys., 20,* 497.

Melrose, D. B. and Dulk, G. A., 1982, *Astrophys. J., 259,* 844.

Melrose, D. B. and Dulk, G. A., 1984, *Astrophys. J., 282,* 308.

Nakajima, H., Dennis, B. R., Hoyng, P., Nelson, G., Kosugi, T., and Kai, K., 1985, *Astrophys. J., 288,* 806.

Ohki, K., and 8 co-authors, 1982, *Proc. Hinotori Symp. Solar Flares,* Tokyo: Inst. of Space and Astronaut. Sci., p. 102.

Tsuneta, S., and 7 co-authors, 1983, *Solar Phys., 86,* 313.

Velusamy, T. and Kundu, M. R., 1982, *Astrophys. J., 258,* 388.

Willson, R. F., 1983, *Solar Phys., 83,* 285.

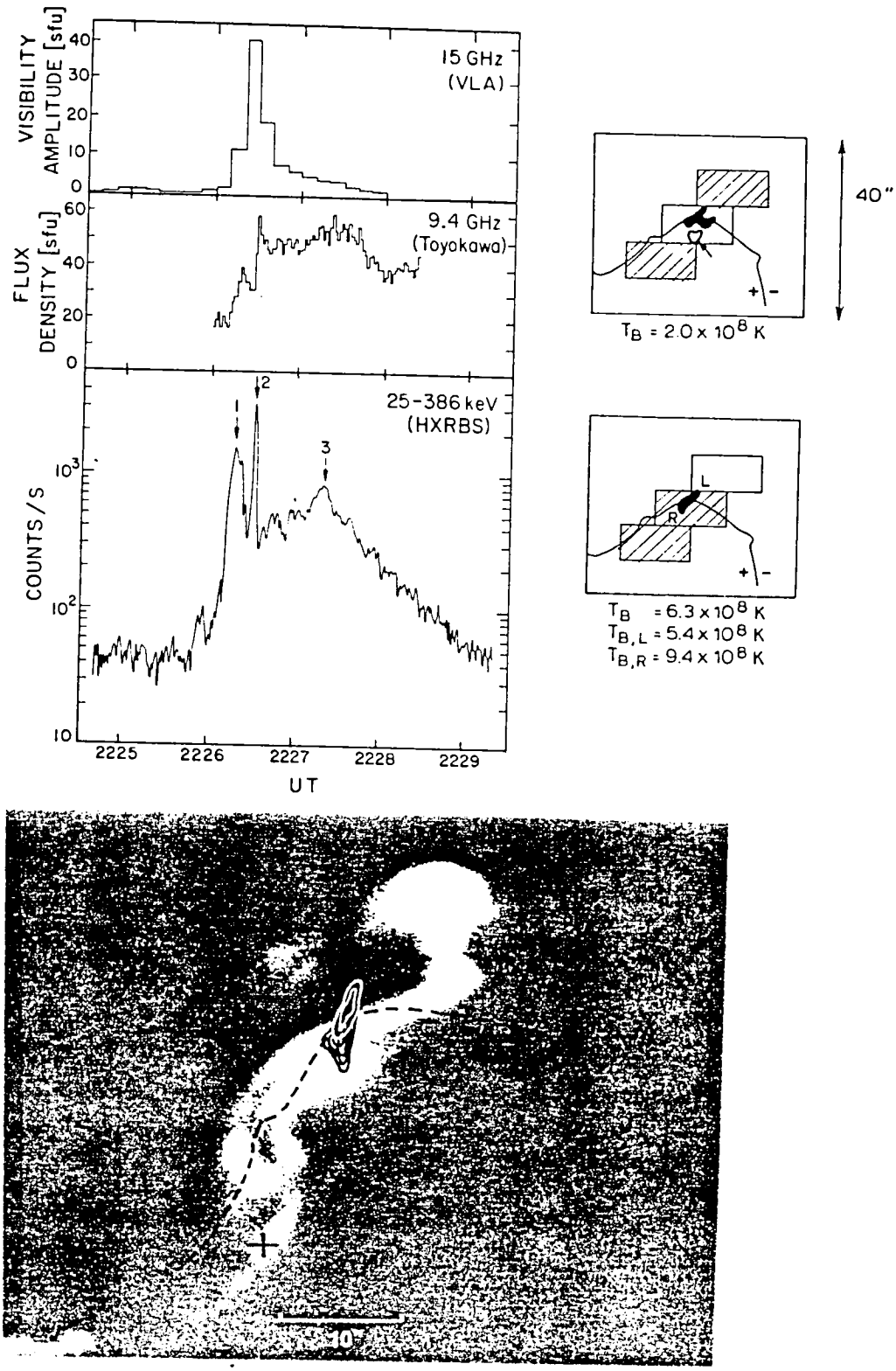

Figure 1. Event of 5 November 1980, 2226 UT. Upper left: light curves at 15 GHz, 9.4 GHz, and 25 - 386 keV X rays. Upper right: images at the times of peaks 1 and 2 of the burst. The solid line represents the magnetic neutral line, the black areas are the 15 GHz sources, and the hatched areas represent HXIS pixels with significant counts in the 16 to 30 keV range. Bottom: superposition of VLA sources in RH (black contours) and LH (white contours) radiation on the Hα picture of the two ribbon flare. From Duijveman and Hoyng (1983) and Hoyng et al. (1983).

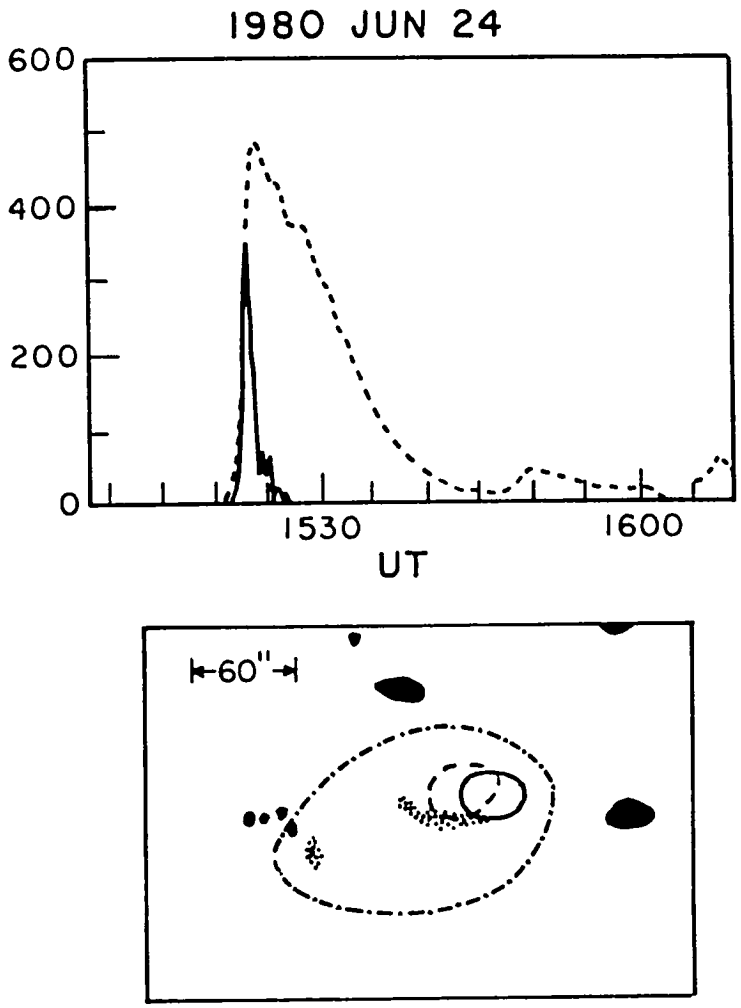

Figure 2. Event of 24 June 1980, 1522 UT. Top: light curves of the soft (3.5 to 8 keV; dotted line) and hard (22 to 30 keV; solid line) X-ray emission. Bottom: positions and sizes of the 5 GHz source (solid curve), hard X-ray source (dashed curve), and soft X-ray source (dot-dash curve) in relation to bright, off-band Hα features (stippled) and sunspots (dark areas) at the time of the peak of the hard X-ray burst. From Kundu et al. (1984).

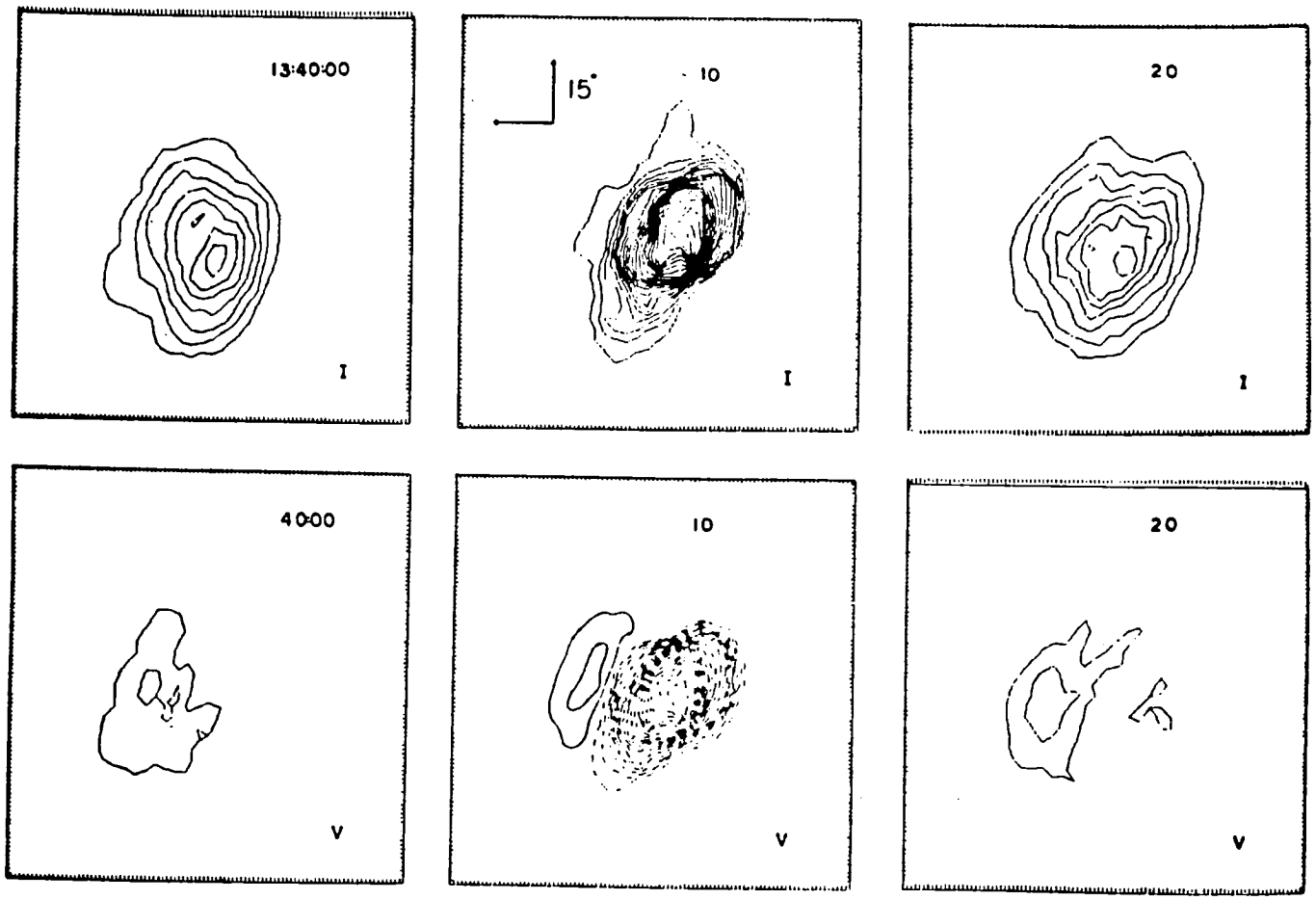

Figure 3. Event of 12 June 1980, 1340 UT. Three successive 10 s VLA maps of intensity (top) and circularly polarized intensity (bottom). Solid and dashed contours represent RH and LH polarization, respectively. From Willson (1983).

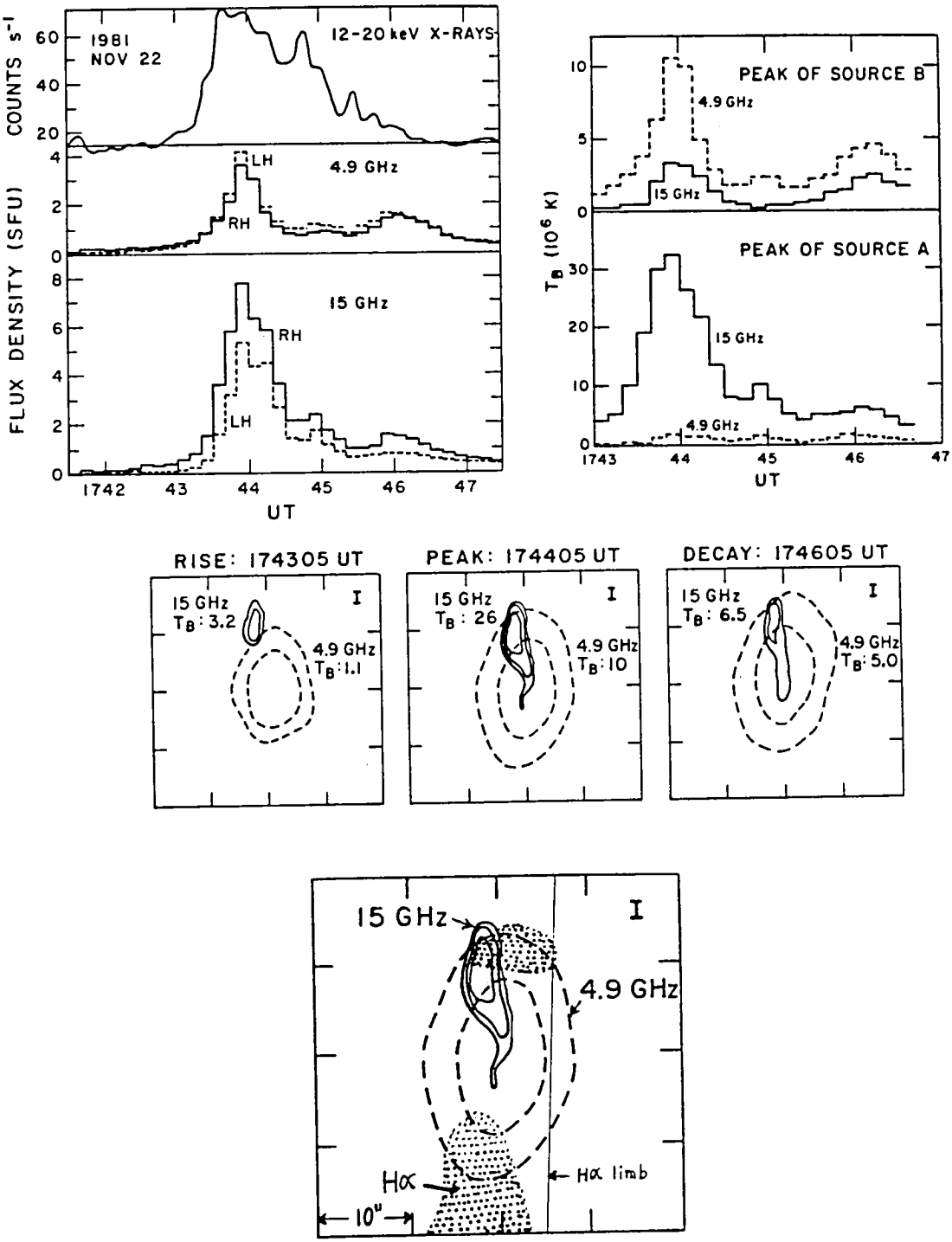

Figure 4. Event of 22 November 1981, 1743 UT. Upper left: light curves of hard X rays and 4.9 and 15 GHz radio waves. Middle: VLA maps of the 4.9 and 15 GHz radio sources at three stages of the flare: rise, first peak, and second peak. Upper right: time variation of the brightness temperature of the RH polarized radiation at the centers of the two sources evident in the middle panel. Bottom: enlarged view of the 4.9 and 15 GHz sources at the time of the first peak, showing their relation with the Hα limb and the bright, flaring Hα features. From Dulk, Bastian, and Kane (1985).

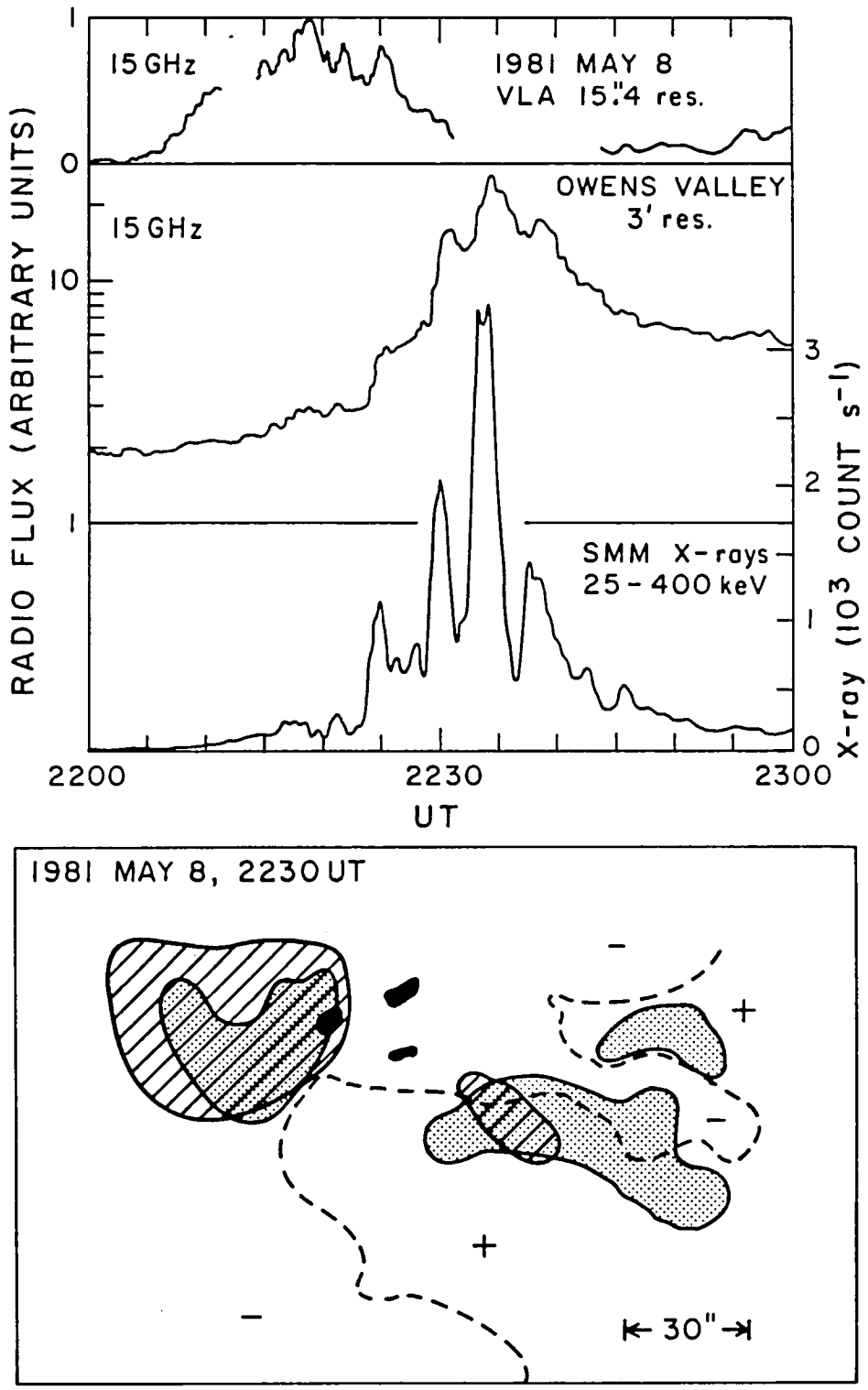

Figure 5. Event of 8 May 1981, 2200 UT. Top: light curves of 15 GHz radiation recorded with a VLA antenna pair with 15.4 arcsecond resolution, 15 GHz radiation recorded with an Owens Valley antenna with 3 ⌒ resolution, and 25 to 500 keV X rays recorded on SMM. Bottom: map of the 17 to 40 keV source structure (shaded areas), its relation to the magnetic neutral line (dashed line), the bright, off-band Hα features (strippled), and three 15 GHz hot spots (dark areas). From Ohki et al. (1982) and Dulk, Bastian, and Hurford (1983).

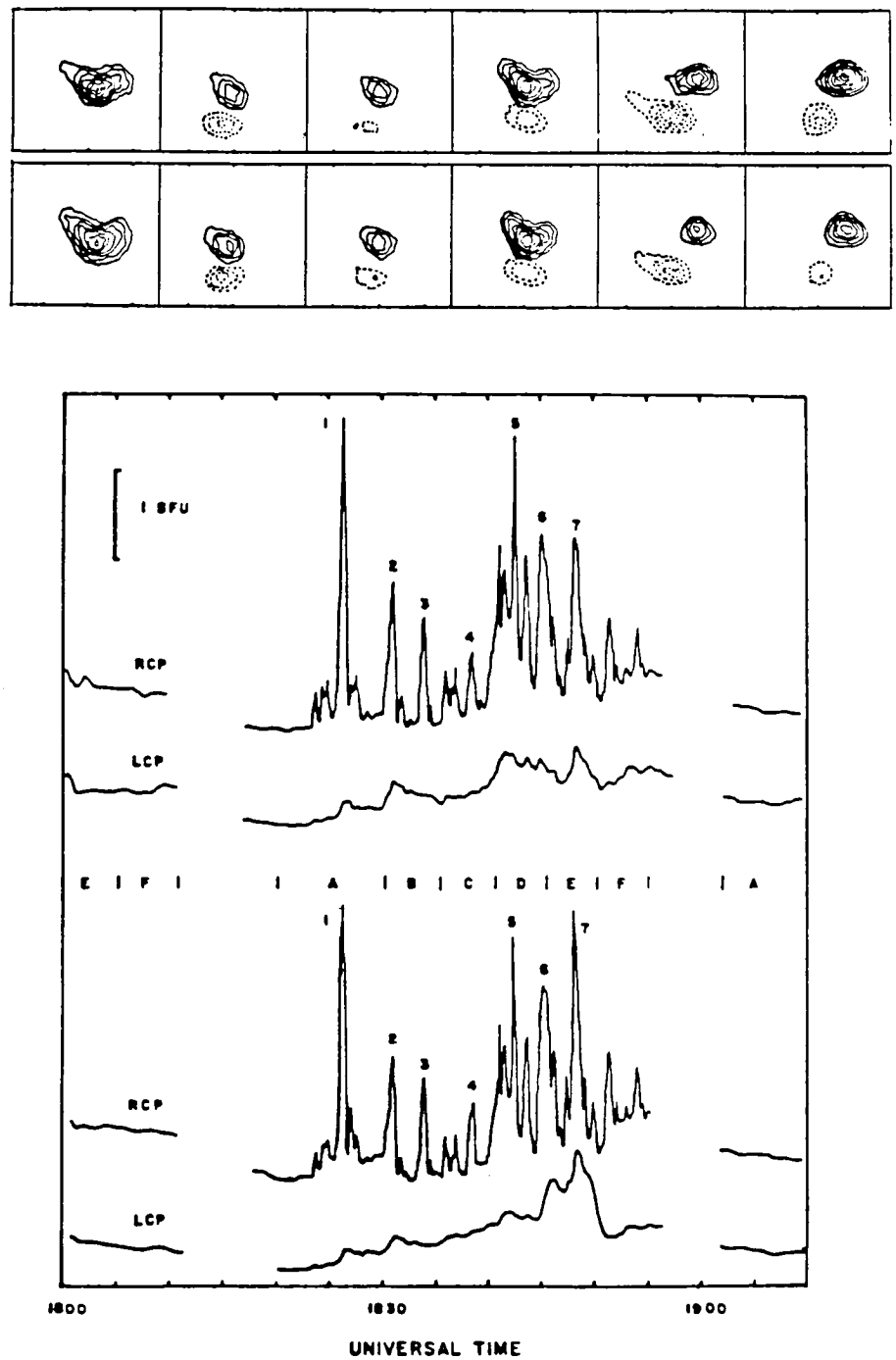

Figure 6. Event of 29 January 1984, 1830 UT. Bottom: a sequence of RH polarized spiky bursts at frequencies near 1.4 GHz. The top and bottom profiles are at closely spaced frequencies, about 30 MHz apart. Both frequencies were changed every 5 min or so, but staying in the range of 1.4 to 1.7 GHz. Top: VLA maps at the times of the seven spikes numbered in the bottom panel. The upper and lower series are for the higher and lower of the closely spaced frequencies, respectively. Solid and dashed contours designate RH and LH polarization, respectively. Peak 7 (far right) has a large difference in brightness temperature at the two frequencies: 1.1×10^8 and 6.0×10^7 K, respectively. The angular scale is shown by the size of the boxes: 16 arcminute square.